

**GA-A22458**

# **AN OVERVIEW OF THE DIII-D PROGRAM**

**by  
J.L. LUXON for the DIII-D TEAM**

**OCTOBER 1996**

GA-A22458

# AN OVERVIEW OF THE DIII-D PROGRAM

by  
J.L. LUXON for the DIII-D TEAM

This is a preprint of a paper to be presented at the 19th Symposium on Fusion Technology September 16-20, 1996, Lisbon, Portugal and to be published in the *proceedings*.

Work supported by  
the U.S. Department of Energy  
under Contract No. DE-AC03-89ER51114

GA PROJECT 3466  
OCTOBER 1996

# AN OVERVIEW OF THE DIII-D PROGRAM

J.L. Luxon for the DIII-D team

## ABSTRACT AND SUMMARY

The DIII-D program focuses on developing fusion physics in an integrated program of tokamak concept improvement. The intent is both to support the present ITER physics R&D and to develop more efficient concepts for the later phases of ITER and eventual power plants. Progress in this effort can be best summarized by recent results for a diverted deuterium discharge with negative central shear which reached a performance level of  $Q_{DT} = 0.32$ . The ongoing development of the tools needed to carry out this program of understanding and optimization continues to be crucial to its success.

Control of the plasma cross-sectional shape and the internal distributions of plasma current, density, and rotation has been essential to optimizing plasma performance. Recent measurements of the current profile have resulted in improved control of the profile and thus significant progress in optimizing the confinement and stability of discharges. Pellet injection along with strong pumping of the plasma edge has provided operation at high plasma density with good confinement. The addition of FWCD and ECH systems is providing the tools needed to develop steady state control of the current and temperature profiles.

Advanced divertor concepts provide edge power and particle control for future devices such as ITER and provide techniques to help manage the edge power and particle flows for advanced tokamak concepts. New divertor diagnostics and improved modeling are developing excellent divertor understanding. Divertor pumping has proven successful at controlling the density and impurity content of plasmas, and the installation of the radiative divertor configuration will allow pumping of the highly shaped configurations which are optimal for high performance. The use of vanadium in parts of the divertor structure will introduce this low activation material into the tokamak environment for the first time.

Many of the plasma physics issues being posed by ITER are being addressed. Scrapeoff layer power flow is being characterized to provide an accurate basis for the design of reactor devices. Ongoing studies of the density limit focus on identifying ways in which ITER can achieve the required densities in excess of the Greenwald limit. Better understanding of disruptions is crucial to the design of future reactors. Measurements of the halo currents have better quantified the spatial and temporal distribution of the currents. Predictive models are being developed to describe the disruption evolution and associated current distributions. The injection of impurity pellets into the edge of a plasma at the onset of a disruption is found to ameliorate the halo currents and heat loads, and a neural network has had success in identifying the onset of disruptions.

## 1. INTRODUCTION

The DIII-D tokamak facility is well-equipped with a diverse set of capabilities and diagnostics to provide germane research both for the development of plasma science and in support of engineering and technology, especially ITER. In recent years, the DIII-D program has focussed on 1) the understanding and efficient use of the divertor configuration, and 2) developing the plasma configuration and internal profiles to optimize tokamak performance including power and particle control.

DIII-D is a non-circular cross-section tokamak with major radius  $R_0=1.66$  m, minor radius  $a=0.66$  m, and plasma chamber elongation of 2.1 with toroidal magnetic field  $B$  of up to 2.2 T at  $R_0$  [1,2]. The tokamak operates in a wide range of

configurations including single null and double null divertors. The maximum plasma current  $I_p$  is presently 2.5 MA. 20 MW of neutral beam heating and 6 MW (source) of fast wave power are routinely available, and 1.0 MW (source) of 110 GHz ECH power has been recently commissioned. The device operates largely in deuterium. DIII-D operation is characterized by highly reproducible discharges due, in part, to the capabilities discussed in this section.

Improvements in the reduction of error fields present at plasma initiation and attention to cleanliness of the vessel walls has resulted in routinely achieving initiation and startup with remarkably low voltages of 3.0 V or less without auxiliary power. This has been aided by the use of helium glow discharge cleaning between tokamak discharges and the occasional boronization of the carbon wall facing

\*Work supported by U.S. Department of Energy under Contract No. DE-AC03-89ER51114.

surfaces. Low voltage startup is significant for next generation devices where a voltage reduction reduces power supply costs.

Development of the digital plasma control system has been effective in providing enhanced capabilities to manage plasma configurations and profiles [3,4]. This system allows superb flexibility in implementing new control algorithms and developing new operating configurations. Recently, the plasma configuration is controlled to match a desired equilibrium configuration using real time MHD equilibrium calculations. This capability has allowed us to implement new plasma configurations and control algorithms including new crescent shaped plasma cross-sections and precise control of the divertor X-point location over a wide range of plasma parameters. A neural network based algorithm to detect conditions leading to disruptions has been developed [5] and installed into the plasma control computer. This system is capable of predicting disruptions due to exceeding the beta limit better than conventional standards such as the Troyon limit.

## 2. HIGH PERFORMANCE DISCHARGES

The achievement of high performance tokamak discharges has been an ongoing commitment of the DIII-D program. Continuous improvement of the performance of tokamak discharges as measured by, i.e., the product of the plasma pressure normalized to the magnetic field and the energy confinement time,  $\beta\tau_E$ , has been demonstrated by exploiting the roles of elongation, triangularity, and shaping of the pressure and current profiles. These improvements, when obtained simultaneously and in steady-state, lead to more cost effective tokamak power plants.

The development of discharges with current profiles modified to be hollow so that the magnetic shear in the central region of the plasma discharge is negative has resulted in discharges with thermonuclear performance well beyond that previously achieved on DIII-D and comparable to that achieved on devices with larger size and higher magnetic fields [6]. The plasma configuration had an elongated triangular cross-section identified as having superior confinement and stability properties. By shaping the current profile transiently using the expeditious application of neutral beam heating early in the discharge, the required hollow current profile was obtained and a discharge with very high central confinement resulted. In the best discharge,  $\tau_E = 0.4$  s ( $4.5 \tau_{ITER89P}$ ) and  $\beta = 6.7\%$  ( $\beta_N = \beta_a B / I_p = 4.0$ ), resulting in values of the fusion reactivity

$Q_{DD} = 0.0015$ . If this reaction rate is projected to DT fuel using a detailed energy transport analysis code and making no correction for isotopic dependence of confinement, the result is  $Q_{DT} = 0.32$ . This is three times the reactivity achieved previously in DIII-D and remarkable compared to the results of larger machines when normalized to the major radius and toroidal field [6].

High performance discharges have been achieved in single-null divertor configurations with lower triangularity ( $\delta = 0.3$ ) and low safety factor ( $q \approx 3$ ) prototypical of high performance JET discharges and of ITER by modifying the plasma internal profiles to produce areas of weak negative central shear and a broad pressure profile [7]. Values of  $\beta_N = 4$  were achieved, comparable to the best previous discharges. The H-mode edge transport and an internal transport barrier presence lead to global energy confinement exceeding ITER-89P by a factor of 4 and fusion reactivity of  $Q_{DD} \sim 1 \times 10^{-3}$ . The performance of the single-null discharges normalized to  $I_p$  is comparable to that achieved in double-null discharges except that higher  $p$  can be achieved with double-null for the same safety factor.

These highest performance single and double-null results are obtained for short durations (0.1 s) owing to the lack of tools for long pulse control of the current and pressure profiles. In single-null discharges with longer duration (1.5 s), performance parameters of  $H = 2.5$  and  $\beta_N = 3.0$  have been achieved. The aim of future experiments will be to use current drive to sustain the optimum profiles.

The presence of negative magnetic shear alone is not sufficient to explain the confinement improvement seen in the discharges described above [8]. The ion energy transport is sharply reduced in the core region to below the neoclassical value, while the electron transport is also reduced to a lesser extent [Fig. 1(a)]. Other characteristics are seen experimentally including the presence of a power threshold and peaking in the ion and electron temperature profiles, and a substantial increase in the core plasma rotation. A likely mechanism for this is the reduction of turbulence driven transport by  $E \times B$  shear decorrelation of turbulence wherein the shear dramatically reduces the turbulent eddies causing the transport [9–11]. Experimental data shows that stabilization by the  $E \times B$  shear increases dramatically as the plasma makes the transition into enhanced confinement, so that it far exceeds the calculated growth rate for the dominant mode in the center of the plasma, in this case the trapped electron  $\eta_i$  mode [Fig. 1(b)] [12]. The incremental radial electric field

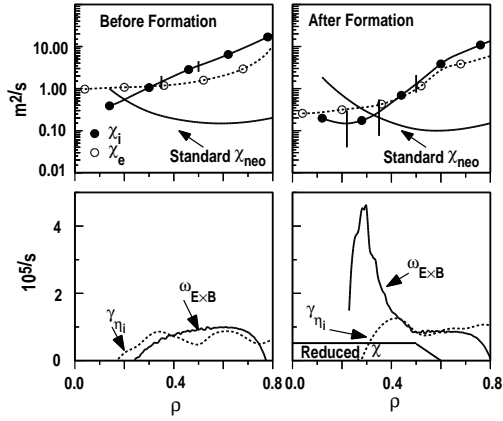


Fig. 1. Transport before and after the transition to negative central magnetic shear. (Top): The ion and electron diffusivity. (Bottom): The calculated growth rate for the (dominant)  $\eta_i$  mode and the damping from  $E \times B$  shear shown on the same scale.

which provides this stabilization comes largely from an increase in the rotation in the plasma core following the stabilization of the MHD modes by the increased negative magnetic shear. Further evidence in support of this comes from the virtual disappearance of core turbulence following the transition [8].

Fast wave current drive (FWCD) offers a means of providing the steady state current profiles needed for these enhanced performance discharges. Experiments using 2.4 MW of fast wave power have successfully demonstrated that fast wave power can be used to broaden the region of negative shear and make the shear more negative Fig. 2 [13]. The previously observed current drive efficiency [ $\eta = n(10^{20}) I(\text{MA}) R(\text{m}) / P(\text{MW})$ ] of FWCD scales with temperature to higher temperature. Analytical models using these results indicate that by using up to 6 MW (source) of 110 GHz ECH heating to heat the electrons in DIII-D along with existing FWCD and neutral beam heating capabilities, that the profiles needed to maintain high performance discharges steady state (10–20 s in DIII-D) could be sustained.

Historically, the densities at which the tokamak could operate appeared limited by physical phenomena collectively characterized by the Greenwald limit ( $n_{\text{max}}^{\text{GW}} \sim I_p / \pi a^2$ ). ITER has identified the advantages of operating at densities above this limit in achieving ignition with successful divertor operation. ITER requirements call for  $n \geq 1.5 n_{\text{max}}^{\text{GW}}$ , with H-mode confinement (H=2),  $q_{95}=3$ , and  $\beta_N=2$ . Experiments on DIII-D have been undertaken to understand the physics of the density limit and devise paths beyond it.

Experiments show there is no fundamental obstacle to achieving densities above the Greenwald limit [14]. Using low neutral-beam-injected power, divertor gas pumping, a progression of regularly spaced deuterium pellets, and stopping pellet injection above a pre-programmed density, we achieved discharges (Fig. 3) with quasi-steady ( $\geq 0.5$  s)

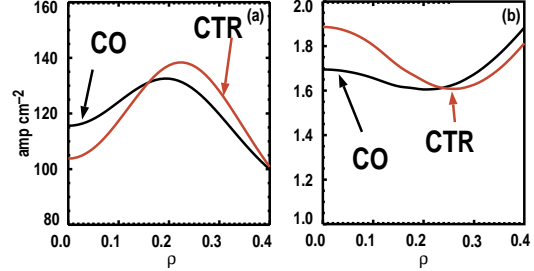


Fig. 2. Comparison of co- and counter-FWCD applied to similar discharges. (a) the current density as a function of the normalized radius in the central region. (b) the resultant profile of the safety factor  $q$ . RF power of 2.4 MW was applied and the data waste taken 400 ms into the rf pulse.

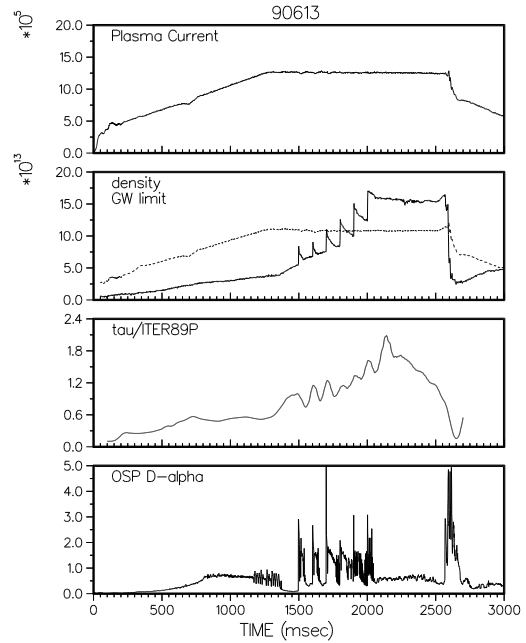


Fig. 3. Pellet injection into an H-mode discharge resulting in density exceeding the density limit. (a) the plasma current, (b) the plasma density and density limit, (c) the confinement time normalized to the ITER-89P confinement scaling, (d)  $D\alpha$  light showing ELM behavior at each pellet and a quiescent period during the high density flat top.

line-average density 40%–60% above  $n_{\max}^{\text{GW}}$ , with global energy confinement times of 1.5–1.8, normalized to ITER89-P scaling. The discharge was ELM-free between pellets, and each pellet triggered an ELM. As the radiated power increased during the ELM-free phase 2.0–2.6 s, the energy confinement time gradually degraded. A H–L transition was observed at  $t=2570$  ms, and a locked mode rapidly ejected particles at  $t\sim 2600$  ms. During the experiments, restrictions on the accessible density window resulted from pellet fueling limits, H–L power transition limit, and MHD activity onset.

### 3. DIVERTOR DEVELOPMENT

Understanding of the plasma wall interaction and, particularly, the divertor is essential to the next-generation device designs and meaningful upgrades of large tokamaks. Two major issues can be identified; control of the particle flow from the plasma edge including impurity and ash removal, and management of the heat flux and erosion at the divertor surface. Progress has been made in both areas.

To understand the physics of the divertor region and plasma surface interactions, it is essential to characterize the plasma properties in this region, along with those of the core plasma and the edge region well away from the divertor where the local properties are determined by the transport from the core. DIII–D has had an outstanding set of core and edge plasma diagnostics. A comprehensive set of divertor diagnostics has been developed to complement these [15], including Thomson scattering, spectroscopy, and probe measurements. Simultaneously, computer models have been developed to relate the measurements to physical understanding [16]. The combination of capabilities is leading to a better understanding of divertor plasma and to improved divertor configurations.

Long-legged divertor configurations have been developed in which much of the plasma energy is radiated away before it reaches the wall and the plasma interacting with the wall is quite cold (Fig. 4). The divertor legs, normalized to the device size are the same length or longer ( $r/a=0.9$ ) than the divertor legs of the present ITER design ( $r/a=0.67$ ). These discharges represent perhaps the closest yet achieved to the proposed ITER design. These partially detached divertors were formed by flowing deuterium gas into the mid-plane region and pumping near the outer divertor leg [17]. These discharges radiate along the entire outer divertor leg, and the heat flux at the divertor surface is reduced a factor of

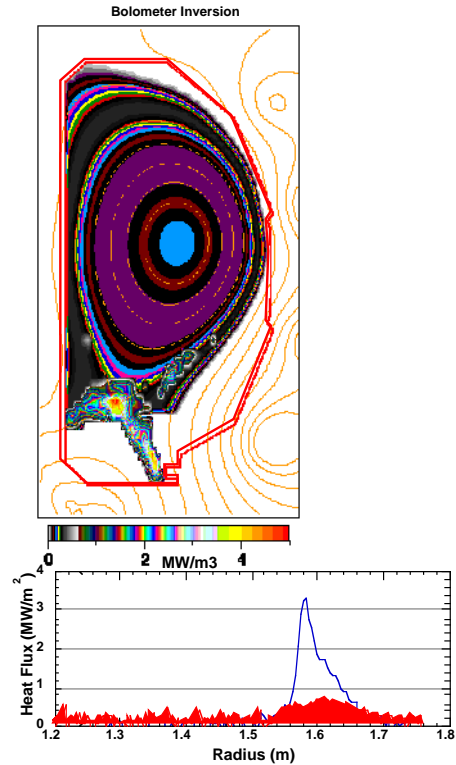


Fig. 4. A reconstruction of the radiated power from a long-legged divertor discharge showing a high level of radiation along the divertor leg following the onset of deuterium injection. Below is the heat flux to the divertor before (line) and after (solid) the radiating zone was established.

3 to 5 while the radiated power increases proportionally. The temperature at the divertor plates is seen to drop to about 1 eV. These low temperatures would substantially reduce the erosion expected in a large steady state fusion device.

The analysis of these discharges is producing reasonable agreement with models [16]. The observed low temperatures at the divertor plate has led to changes in the physics models used to describe the divertor region. In particular, more atomic processes, such as volumetric recombination, were included. The model correctly shows the long cool region of high radiation along the divertor leg and the low temperatures at the divertor plate.

### 4. DISRUPTIONS

The understanding of disruptions is crucial to the design of next-generation tokamaks. The DIII–D

program has taken a strong role in understanding the disruption process, characterizing and modeling disruptions and developing techniques to mitigate disruptions [18].

The heat pulse and the halo currents from the disruption have been characterized. Heat flux measurements during high beta and impurity-induced disruptions have shown that 70%–90% of the energy lost is incident on the divertor region. The peak of the energy distribution is often far from either of the divertor strike points and can move substantially during the disruption. The width of the heat pulse distribution on the divertor plates can range from as little as 3 cm to as much as 10 cm (FWHM).

Halo currents are poloidal currents flowing from the plasma mantle through the vessel wall components and back into the mantle during the transient conditions of a disruption. Understanding of the halo currents has evolved considerably in the last year with the availability of improved diagnostics. Under combined worst case conditions, halo currents of as much as 30% of the total plasma current are observed in DIII–D and the toroidal asymmetries in these currents can be as large as a factor of two at the peak currents [18]. Higher asymmetries have been seen, but only at proportionally less total halo current. On time scales of less than a millisecond, yet higher transient values of the current (40% of  $I_p$ ) and peaking factor (5) have been seen, but the time scale is so fast they are of little significance to the engineering of DIII–D.

The injection of impurity pellets at the onset of a disruption has been found to significantly mitigate the consequences of disruptions [19]. Neon pellets with diameters of 1.7 and 2.8 mm (up to 20 percent of the plasma particles) were injected into both discharges with triggered vertical displacement events and into normal stable discharges (Fig. 5). The pellets caused 70% of the thermal energy to be lost by the end of the pellet ablation. The current decay begins within 1 ms of the end of the ablation and the halo currents were found to decrease by a factor of two compared to disruptions without pellets injected. There was also very little asymmetry in the halo currents observed under these conditions. Small amounts of runaway electrons were seen following the pellet injection which is significant because runaway electrons were not seen in disruptions of similar discharges without pellet injection and are not normally seen in disruptions of DIII–D discharges. The presence of runaways is consistent with the Dreicer condition for electron avalanche.

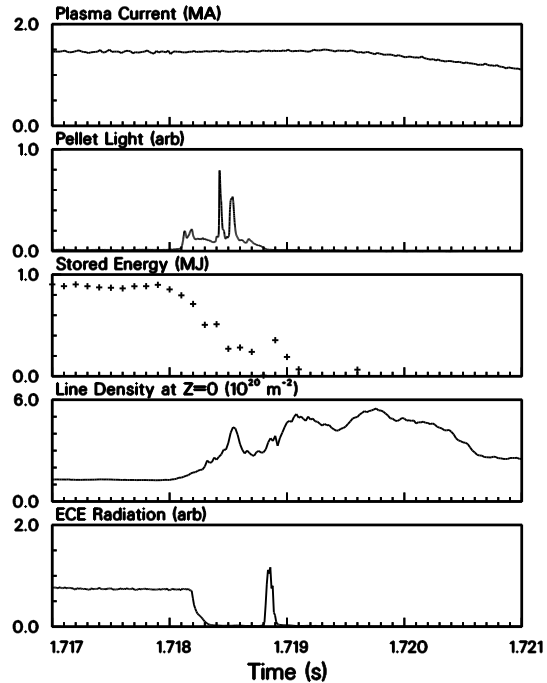


Fig 5. Data from neon pellet injection into a discharge undergoing a vertical displacement event. The discharge began at  $\sim 0$  on the time scale. (a) plasma current, (b) pellet light indicating ablation takes place in  $\sim 0$ – $0.75$  ms, (c) plasma stored energy, (d) plasma density, (e) electron cyclotron emission indicating the presence of a runaway tail at 1718.8 s. The emission is non-thermal in character.

## 5. FUTURE PLANS

Better understanding of divertor configuration has led to the need for a more closed divertor to inhibit recycling of divertor neutrals back to the edge of the main plasma. Understanding of the role of the plasma configuration in the accessibility of high performance regimes has indicated the need for a more triangular cross-section for the diverted plasmas. This has led us to develop the Radiative Divertor configuration, the first phase of which is being installed in the DIII–D vessel in the fall of 1996 [20,21]. This configuration will allow us to directly compare triangular divertors formed using the top divertor with the presently achievable less triangular shapes using the lower divertor while allowing us to maintain the excellent diagnostic capabilities of the lower divertor. Future activities, if supported by experimental results, will be to install a second divertor for the lower null of the triangular

configuration and re-establish the detailed divertor diagnostic for this new configuration.

One of the major problems facing development of fusion power plants is the availability of low activation materials especially metals for the fabrication of structural components. One of the best candidate metals is vanadium which when activated by neutron bombardment substantially decays in 10 years. This metal is abundant, but suitable fabrication techniques are not well developed. General Atomics and the DIII-D program has begun a program of developing vanadium fabrication techniques which will culminate in the fabrication and installation of vanadium components in the second phase of the Radiative Divertor Program [22].

As discussed, additional ECH power is key to achieve steady-state the profiles needed for high performance advanced tokamak discharges. A total of 3 MW (source) of ECH power is planned next year with an additional 3 MW (source) planned later.

## REFERENCES

- [1] J.L. Luxon, *Fusion Engr. Des.* **30** (1995) 39.
- [2] J.L. Luxon and L. Davis, *Fusion Technol.* **8** (1985) 441.
- [3] M.L. Walker, *et al.*, *Proc. 16th Symp. on Fusion Engineering*, Champagne, Illinois (1995) 885.
- [4] B.G. Penaflo, *et al.*, "A Structured Architecture for Advanced Plasma Control Experiments," this conference.
- [5] D. Wroblewski, G.L. Jahns, and J.A. Leuer, "Tokamak Disruption Alarm Based on a Neural Network Model of the High Beta Limit," submitted to *Nucl. Fusion*.
- [6] E.A. Lazarus, "Higher Fusion Power Gain with Profile Control in DIII-D Tokamak Plasmas," submitted to *Nucl. Fusion*.
- [7] E.J. Strait, *et al.*, "Improved Fusion Performance in Low-q, Low Triangularity Plasmas with Negative Central Shear," *Proc. 23rd Euro. Conf. on Contr. Fusion and Plasma Phys.*, Kiev, Ukraine, 1996 (European Physical Society, Petit-Lancy, Switzerland) to be published.
- [8] L.L. Lao, *Phys. Plasmas* **2** (1995).
- [9] Hahn, Burrell, *Phys Plasmas* **2** (1995) 1648.
- [10] P.H. Diamond, *et al.*, submitted to *Phys. Rev. Lett.*
- [11] F.L. Hinton and G.M. Staebler, *Phys. Fluids B* **5** (1993) 1281.
- [12] E.J. Strait, *Phys. Rev. Lett.* **75** (1995) 4421.
- [13] R. Prater, *et al.*, "Fast Wave Discharges and Current Drive in DIII-D in Discharges with Negative Central Shear," *Proc. 16th International Conf. Plasma Phys. and Contr. Nucl. Fusion Research*, Montreal, Canada, 1996 (International Atomic Energy Agency, Vienna, Austria) to be published.
- [14] R. Maingi, *et al.*, "Investigation of the Physical Processes Limiting Plasma Density in DIII-D," to be published in *Phys. Plasmas*.
- [15] S.L. Allen, "Recent Results from Tokamak Divertor Plasma Measurements," *Proc. 11th Topical Conf. High Temperature Plasma Diagnostics*, Monterey, California, (1996).
- [16] G.D. Porter, *et al.*, "Divertor Characterization Experiments and Modeling in DIII-D," *Proc. 23rd Euro. Conf. on Contr. Fusion and Plasma Phys.*, Kiev, Ukraine, 1996 (European Physical Society, Petit-Lancy, Switzerland) to be published.
- [17] A.W. Leonard, *et al.*, "Divertor Heat and Particle Flux Due to ELMs in DIII-D and ASDEX-Upgrade," *Proc. 12th International Conf. on Plasma Surface Interactions in Contr. Fusion Devices*, Saint Raphael, France (1996) to be published.
- [18] A.G. Kellman, *et al.*, "Disruptions in DIII-D," *Proc. 16th International Conf. Plasma Phys. and Contr. Nucl. Fusion Research*, Montreal, Canada, 1996 (International Atomic Energy Agency, Vienna, Austria) to be published.
- [19] T.E. Evans, *et al.*, "Measurements of Non-axisymmetric Halo Currents With and Without "Killer" Pellets During Disruption in the DIII-D Tokamak," *Proc. 12th International Conf. on Plasma Surface Interactions in Contr. Fusion Devices*, Saint Raphael, France (1996) to be published.
- [20] S.L. Allen, *et al.*, "First Measurements of Electron Temperature and Density with Divertor Thomson Scattering in Radiative Divertor Discharges on DIII-D," *Proc. 12th International Conf. on Plasma Surface Interactions in Contr. Fusion Devices*, Saint Raphael, France (1996) to be published.
- [21] E.E. Reis, *et al.*, "Structural Design of the DIII-D Radiative Divertor," this conference.
- [22] J.P. Smith, *et al.*, "Fabrication Development and Usage of Vanadium Alloys in DIII-D," this conference.